VIP The following Communications have been judged by at least two referees to be "very important papers" and will be published online at www.angewandte.org soon:

Author Profile

"When I was eighteen I wanted to be a mechanical engineer.
The biggest challenge facing scientists is nonlinearity …"
This and more about Younan Xia can be found on page 6958.

Highlights

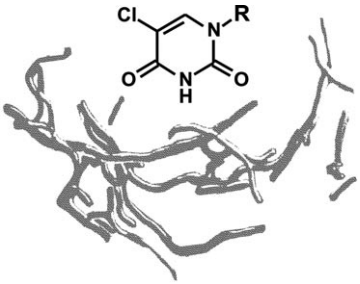

An automated system for the continuous cultivation of cells in suspension has been used to globally change the composition of the DNA genome of *E. coli*. Thymine was replaced almost completely by 5-chlorouracil through artificial evolution of cells, during which the bacterial genome accumulated hundreds of mutations under permanent conditions of proliferation and selection. The resulting 5-chlorouracil-adapted descendants had the ability to grow on 5-chlorouracil.

Organism Chemistry

Contents

The full picture: In a new strategy for catalyst design, the coupling of steric and stereoelectronic differentiation to develop the salalen–titanium complex pictured resulted in one of the highest degrees of stereocontrol ever observed for the production of isotactic polypropene (*i*PP). Ad = adamantyl, Bn = benzyl.

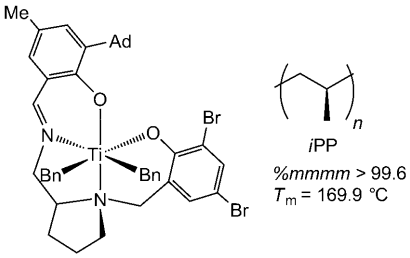

Reviews

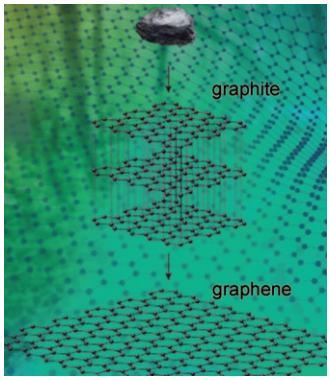

There can be only one: In their Nobel Reviews, the laureates tell the story about the ever changing, exciting scientific pathways that eventually—for example, with the aid of simple adhesive tape—led them to the discovery of graphene. Graphene is a carbon monolayer with almost magical abilities, including exceptional strength, stability, and electronic properties, with massless Dirac fermions as charge carriers.

Communications

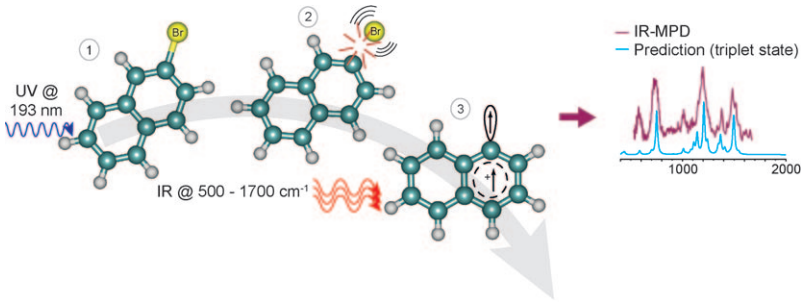

Run to ground: Infrared spectroscopy of the isolated naphthyl carbocation, $C_{10}H_7^+$ (prepared from $C_{10}H_7Br$, see scheme) provides evidence for a triplet electronic ground state ($^3A''$), in which a π electron is promoted to the vacant σ orbital. Previous computational studies have been ambiguous as to the relative stabilities of the singlet and triplet states; DFT calculations predict both states to be practically isoenergetic.

For the USA and Canada:
ANGEWANDTE CHEMIE International Edition (ISSN 1433-7851) is published weekly by Wiley-VCH, PO Box 191161, 69451 Weinheim, Germany. Air freight and mailing in the USA by Publications Expediting Inc., 200 Meacham Ave., Elmont, NY 11003. Periodicals postage paid at Jamaica, NY 11431. US POSTMASTER: send address changes to *Angewandte Chemie*, Journal Customer Services, John Wiley & Sons Inc., 350 Main St., Malden, MA 02148-5020. Annual subscription price for institutions: US$ 9442/8583 (valid for print and electronic / print or electronic delivery); for individuals who are personal members of a national chemical society prices are available on request. Postage and handling charges included. All prices are subject to local VAT/sales tax.

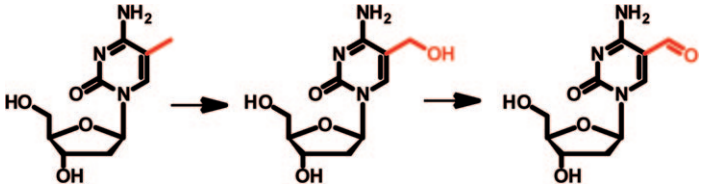

Touching base: Sophisticated mass spectrometry has shown that 5-formylcytosine is a constituent of mammalian embryonic stem cell DNA. This base is likely produced from methylcytosine via hydroxymethylcytosine (see scheme), and it may serve as an intermediate in the long searched for pathway of active DNA demethylation.

Bioorganic Chemistry

Nine in a line: A multifaceted approach, including a silylethylene functionalization strategy, to the synthesis of stable nonacene derivatives (see picture, F green, Si blue) allows an unprecedented level of characterization, including electrochemical, photophysical, and crystallographic studies. The nonacenes show a strong S_0–S_1 transition and no fluorescence in the visible region.

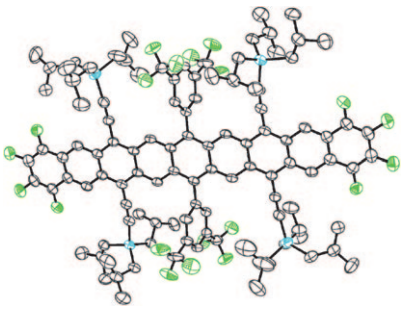

Oligoacenes

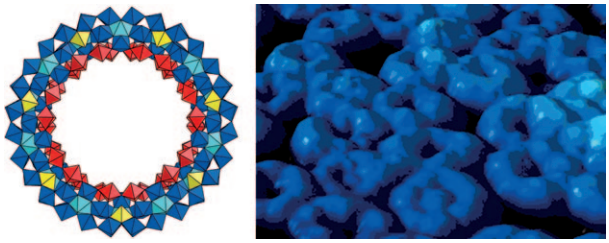

The electrons go in two by two: Scanning tunneling microscopy (STM)/spectroscopy (STS), shows the Mo_{154} giant wheel cluster to have a unique localization of states within each of the 14 identical compartments forming its necklace-type structure (see picture). Each compartment contains two delocalized electrons. These states make the system different from conventional quantum dots that have completely free electrons or excitonic states.

Polyoxometalate Necklace

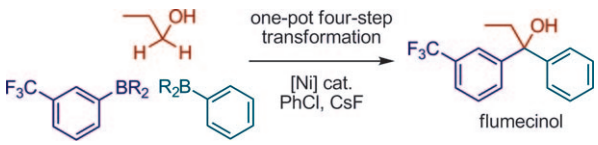

All in one pot: A general synthetic platform allows the interconversion of alcohols and carbonyl compounds in a predictable and controlled fashion in one pot. Under the action of a Ni catalyst, PhCl, CsF, and arylboronates, several multistep alcohol–carbonyl interconversions have been achieved with good overall efficiency (see scheme). A one-pot nickel-catalyzed synthesis of flumecinol (a hepatic microsomal enzyme inducer) has also been demonstrated.

Alcohol–Carbonyl Interconversion

Contents

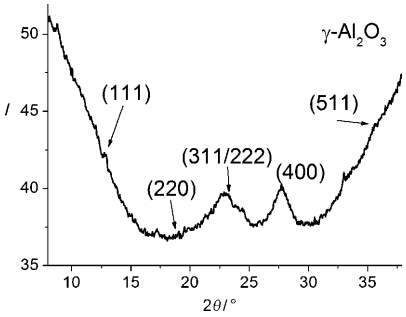

Alumina in flow: Information obtained from in situ synchrotron powder X-ray diffraction (PXRD) measurements was used to develop the first large-scale, rapid, one-step synthesis of γ-Al_2O_3. The data suggest a reaction mechanism that does not involve crystalline intermediates, and γ-Al_2O_3 was prepared at low temperature in a continuous-flow reactor using aluminum isopropoxide in 2-propanol/water without subsequent calcination.

Nanoparticles

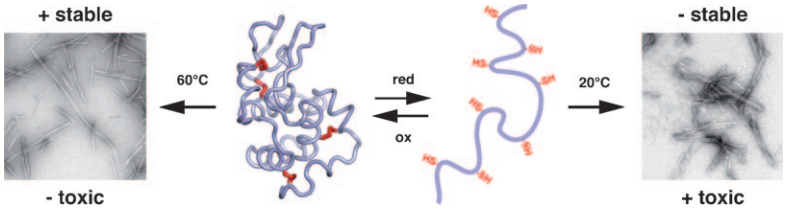

In a stable condition: Disulfide bonds stabilize folded proteins primarily by decreasing the entropic cost of folding. Such cross-links also reduce toxic aggregation by favoring the formation of highly structured amyloid fibrils (see picture). It is suggested that disulfide bonds in extracellular proteins were selected by evolutionary pressures because they decrease the propensity to form toxic aggregates.

Amyloid Toxicity

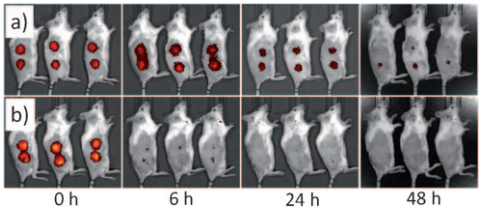

Amphiphilic oligonucleotides synthesized by covalent conjugation between a hydrophobic diacyllipid tail and chemically stabilized RNA or DNA oligonucleotides can directly label tumor cells on injection into solid tumors. In a murine melanoma tumor model, cell membrane-anchored CpG ODNs with a nuclease-resistant phophorothioate backbone (row a) exhibited significantly enhanced immunostimulatory activity compared to soluble CpG (row b).

Sticky Oligonucleotides

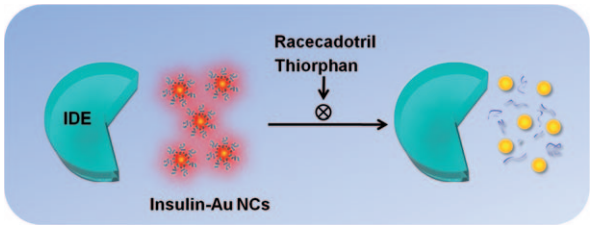

Go for gold: As-prepared insulin–Au nanoclusters (NCs) show intense red fluorescence, excellent biocompatibility, and preservation of natural insulin bioactivity in lowering the blood-glucose level. Their versatility in applications is demonstrated by fluorescence imaging, X-ray computed tomography, and insulin–inhibitor interactions (see picture; IDE = insulin-degrading enzyme).

Gold Nanoclusters

Contents

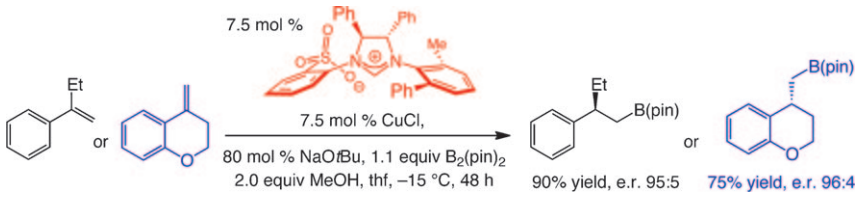

Tough nut to crack: Chiral bidentate N-heterocyclic carbene copper complexes were designed that promote enantioselective hydroborations of one of the most difficult substrate classes: acyclic and exocyclic 1,1-disubstituted alkenes undergo reaction with >98% site selectivity, in up to >98% yield and e.r = 96.5:3.5 (see scheme, $B_2(pin)_2$ = bis(pinacolato)diboron).

Enantioselective Catalysis

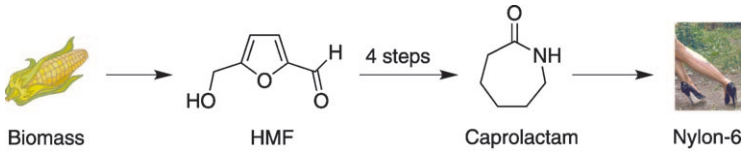

Renewable nylon: 5-Hydroxymethylfurfural (HMF), which can be obtained from renewable resources such as D-fructose, was converted into caprolactone with very good overall selectivity in only three steps. The new route involves two hydrogenation steps to obtain 1,6-hexanediol, which was oxidatively cyclized to caprolactone, and then converted into caprolactam.

Sustainable Chemistry

Nicely decorated: A sandwich-structured photocatalyst shows an excellent performance in degradation reactions of a number of organic compounds under UV, visible light, and direct sunlight (see picture). The catalyst was synthesized by a combination of nonmetal doping and plasmonic metal decoration of TiO_2 nanocrystals, which improves visible-light activity and enhances light harvesting and charge separation, respectively.

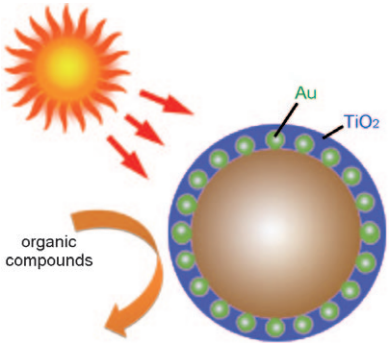

Photocatalysts

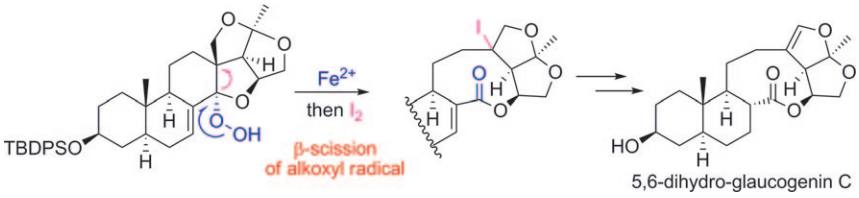

A skeleton key: A biomimetic synthesis of the title natural product was completed in 19 steps and 6.4% overall yield. Iron(II)-promoted fragmentation of α-alkoxy hydroperoxide and subsequent trapping of the resulting tertiary carbon radical by iodide enabled the highly efficient construction of the challenging 13,14:14,15-disecopregnane skeleton (see scheme; TBDPS = *tert*-butyldiphenylsilyl).

Natural Product Synthesis

Contents

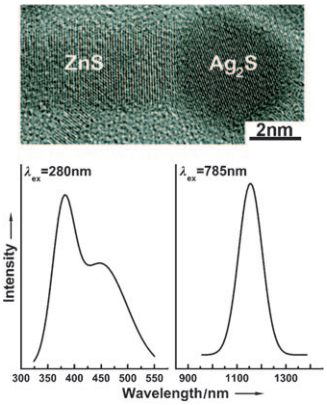

Heterostructured semiconductor matchsticks with Ag_2S heads and ZnS stems (see TEM image) were synthesized by thermal co-decomposition of Ag(DDTC) and $Zn(DDTC)_2$ (DDTC = diethyldithiocarbamate). The heterononanostructures show both UV/blue (λ_{ex} = 280 nm) and near-infrared (λ_{ex} = 785 nm) photoluminescence.

Heteronanostructures

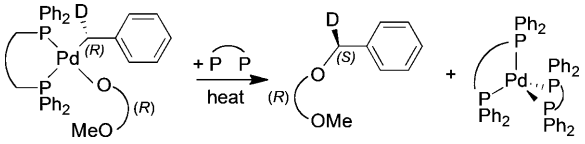

On the contrary: Isolated benzylpalladium aryloxide complexes undergo C(sp^3)–O bond-forming reductive elimination by a stepwise ionic mechanism (see scheme) distinct from the accepted concerted pathway for reductive elimination of aromatic ethers from arylpalladium(II) species. The mechanism is proposed to result from dissociation of the aryloxide ligand followed by nucleophilic attack on the benzylic carbon atom.

C–O Bond Formation

Putting the heat on: Drugs that are essentially inactive at 37 °C and are active under mild hyperthermia can be synthesized by modification of chlorambucil with thermoresponsive groups (see picture; C gray, Cl green, F yellow, H white, N blue, O red). This modification should allow this cytotoxic agent to be used in a more targeted fashion, and consequently, with reduced side-effects.

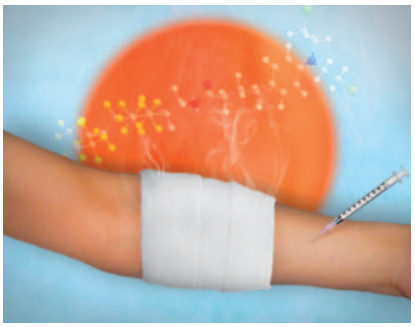

Antitumor Agents

Look both ways: Coordination bonding of verdazyl radicals to diamagnetic metal ions dramatically modifies the crystal packing of the electronic spin bearers. The face-to-face positioning of two radicals leads to a magnetic behavior that is more relevant to a $S = 0$ to $S = 1$ spin-transition phenomenon than to the usual exchange-interaction view.

Spin Transitions

Contents

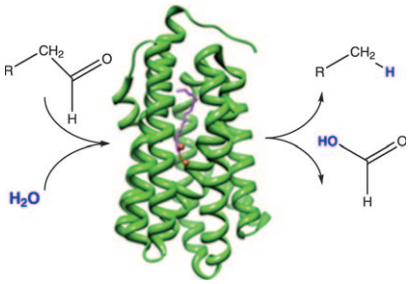

Just add water: Structurally, cyanobacterial aldehyde decarbonylases are members of the non-heme diiron oxygenase family of enzymes. However, the enzyme catalyzes the hydrolysis of aliphatic aldehydes to alkanes and formate (see scheme), in an oxygen-independent reaction. This unusual and chemically difficult reaction most likely involves free radical intermediates.

Enzymology

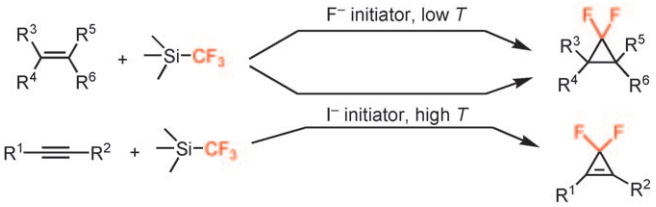

Highly versatile: The Ruppert–Prakash reagent (Me_3SiCF_3) can be an efficient source of difluorocarbene. By varying the nonmetallic initiator that is used (F^- at lower temperatures and I^- at higher temperatures), a range of structurally diverse alkenes and alkynes can be converted into the corresponding *gem*-difluorinated cyclopropanes and cyclopropenes in good yields (see scheme).

Fluorine Chemistry

Changing behavior: A nucleophilic sp^2 carbene-type boryl moiety, formed upon interaction of tetraalkoxydiboranes and a Lewis base, can attack non-activated C=C bonds. Computational studies identify the interaction as the overlap between the strongly polarized B–B σ bond (HOMO) and the antibonding π* orbital (LUMO) of the C=C bond. Conceptually, the normally electrophilic boron becomes nucleophilic and forces the olefin to act as an electrophile.

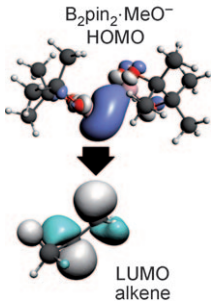

Boron Chemistry

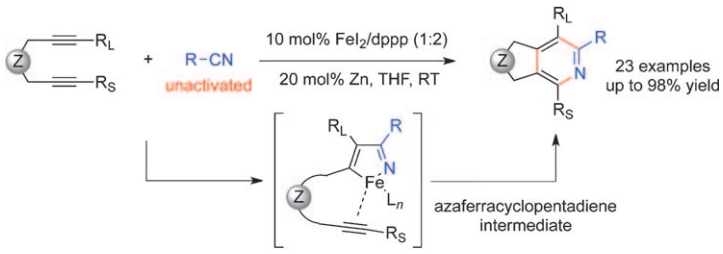

Joined by iron: The iron catalyst for the formation of pyridines at room temperature (see scheme), which was generated in situ from an inorganic iron salt and a diphosphine ligand, exhibited high reactivity and regioselectivity.

[2+2+2] Cycloaddition

Contents

Frustrated, but not frustrating: Frustrated Lewis pairs (FLPs) can undergo selective 1,4-addition reactions with conjugated ynones (see scheme). Upon FLP dihydrogen activation selective hydrogenation of the carbon–carbon triple bond can be achieved, in one case even catalytically.

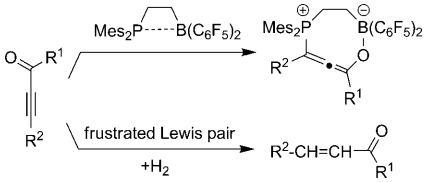

Frustrated Lewis Pairs

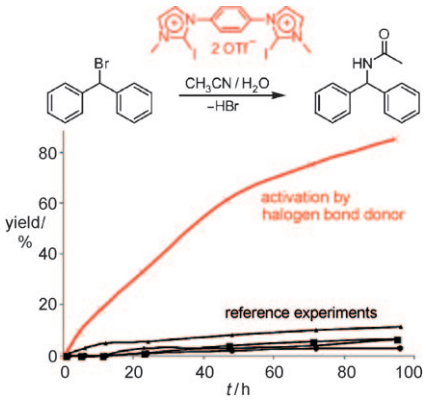

I···Br-idging: Benzhydryl bromide can be activated by novel halogen-bond donors and subsequently undergoes a Ritter-like reaction with acetonitrile (see scheme). Comparative experiments with non-iodinated reference compounds and tests with added acids indicate that halogen bonds are very likely the basis for this effect. The activation seems to be applicable to other substrates as well.

Halogen Bonds

Supporting information is available on www.angewandte.org (see article for access details).

A video clip is available as Supporting Information on www.angewandte.org (see article for access details).

This article is available online free of charge (Open Access)

Service

Contents

Corrigendum

Angew. Chem. Int. Ed. **2010**, *49*

DOI 10.1002/anie.201002906

The authors of this Communication have recognized an error in Figure 1 d and Table 1. Because of an error in the scaling of the NOE values for the MCoTI-I/trypsin complex (Figure S2 C and D in the Supporting Information), the reported S^2 values for the MCoTI-I/trypsin complex were not accurate. The correct Figure 1 and Table 1 are shown below.

The text that refers to Figure 1 d and Table 1 (page 7032, left column) is also inaccurate. It should read: "Thus, although loop 1 showed $\langle S^2\rangle = 0.75 \pm 0.29$, which is slightly lower than the value for the rest of the molecule ($\langle S^2\rangle = 0.78 \pm 0.23$), Lys^4 showed a significant lower value of S^2 upon complex formation. Several other residues in loop 2 (Cys^9), loop 5 (Cys^{27} and Arg^{22}), and loop 6 (Val^1) also showed significantly lower values of S^2 upon complex formation (Figures 1 d and 2 c). It is likely that the increase in mobility observed in these loops may help to accommodate the increased flexibility of Lys^4 in the binding loop (Figure 2 c).

Since our data clearly shows that backbone flexibility of MCoTI-I cyclotide increases in some of the MCoTI-I residues upon binding to trypsin, we decided to estimate the contribution of these motions to the overall Gibbs free energy of binding (ΔG). The energetic benefit of this increase in backbone flexibility can be estimated from the experimental relaxation data, by using the experimentally measured order parameters, S^2.[27] The estimated ΔG value was approximately 10 kJ mol^{-1} at 298 K. This value should be compared to the calculated value from the trypsin inhibitory constant of MCoTI-I (the trypsin inhibitory constant of MCoTI-I ($K_i \approx 20$ pM,[28] $\Delta G \approx -61$ kJ mol^{-1}). The calculated entropic contribution ($-T\Delta S$) at the same temperature was approximately 7 kJ mol^{-1}."

We have also included modified versions of Figure S2 C and D (showing corrected NOE enhancements and R_{ex} values for the MCoTI/trypsin complex), which are included as Supporting Information. The authors would like to point out that this error does not affect the overall interpretation of the results in the Communication.

[27] A. G. Palmer III, *Annu. Rev. Biophys. Biomol. Struct.* **2001**, *30*, 129.
[28] O. Avrutina, H. U. Schmoldt, D. Gabrijelcic-Geiger, D. Le Nguyen, C. P. Sommerhoff, U. Diederichsen, H. Kolmar, *Biol. Chem.* **2005**, *386*, 1301.

Table 1: Average order parameters of structural elements in MCoTI-I in the free state and bound to trypsin.

Structural element	Sequence	$\langle S^2\rangle$[a] Free MCoTI-I	$\langle S^2\rangle$[b] Trypsin–MCoTI-I
loop 1	3–8	0.81 ± 0.01	0.75 ± 0.29
loop 2	10–14	0.81 ± 0.01	0.93 ± 0.04
loop 3	16–18	0.84 ± 0.02	0.82[c]
loop 4	20	0.88[c]	0.98[c]
loop 5	22–26	0.92 ± 0.02	0.80 ± 0.24
loop 6	28–34	0.76 ± 0.05	0.71 ± 0.34
cystine knot	2,9,15,19,21,27	0.84 ± 0.02	0.62 ± 0.33

[a] S^2 values for residues 5 and 23 from free MCoTI-I are not included in the average because the relaxation data could not be fitted to a monoexponential function. [b] S^2 values for residues 2, 5, 8, 18, 19, 23, 29, 31, 32, and 33 from trypsin-bound MCoTI-I are not included in the average because of the lack of signal intensity or because the relaxation data could not be fitted to a monoexponential function. [c] $\langle S^2\rangle$ contains the S^2 value for a single residue.

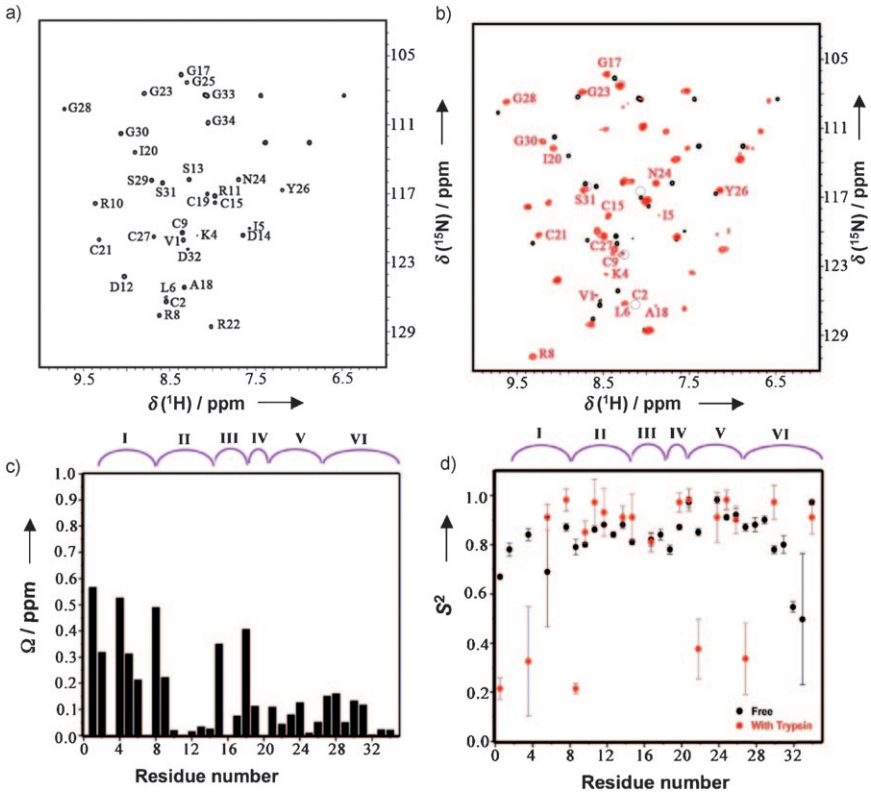

Figure 1. NMR analysis of the backbone dynamic of free and trypsin bound MCoTI-I. a) $\{^{15}N,^{1}H\}$NMR heteronuclear single quantum correlation (HSQC) spectrum of free MCoTI-I. Chemical shift assignments of the backbone amides are indicated. b) Overlay of the $\{^{15}N,^{1}H\}$ HSQC spectra of free (black) and trypsin bound MCoTI-I (red). Residues with large average amide chemical shift differences between two different states (>0.3 ppm) are indicated. Peaks that are broadened in trypsin bound MCoTI-I are indicated by grey circles. c) Average amide chemical shift difference for all the assigned residues in free and trypsin bound MCoTI-I. Chemical shift difference was calculated as: $\Delta\Omega = [(\Delta\Omega^2_{NH} + 0.04\,\Delta\Omega^2_{N})/2]^{1/2}$, where $\Delta\Omega_{NH}$ and $\Delta\Omega_{N}$ are the changes in the amide proton and nitrogen chemical shifts (ppm), respectively. d) Order parameter, S^2, for the free (black) and the trypsin bound MCoTI-I (red). The S^2 value is a measure of backbone flexibility and represents the degree of angular restriction of the N–H vector in the molecular frame. The MCoTI-I loops are shown on top of panels (c) and (d). Small unassigned peaks in the spectra of both free and trypsin-bound of MCoTI-I are from a minor conformation of the protein, and result from a known isomerization of the backbone at an Asp-Gly sequence in loop 6 of MCoTI-I.